Identification of bipolar disorder using a combination of multimodality magnetic resonance imaging and machine learning techniques

Hao Li
Sun Yat-sen University First Affiliated Hospital
Liqian Cui (cui_sysu@163.com)
Sun Yat-sen University First Affiliated Hospital
Liping Cao
Guangzhou Huiai Hospital
Yizhi Zhang
Guangzhou Huiai Hospital
Yueheng Liu
Second Xiangya Hospital
Wenhao Deng
Guangzhou Huiai Hospital
Wenjin Zhou
Guangzhou Huiai Hospital

Research article

Keywords: Bipolar disorder, multimodality imaging, magnetic resonance imaging, support vector machine

Posted Date: February 28th, 2020

DOI: https://doi.org/10.21203/rs.3.rs-15480/v1

Version of Record: A version of this preprint was published on October 6th, 2020. See the published version at https://doi.org/10.1186/s12888-020-02886-5.

Abstract

Background Bipolar disorder (BPD) is a common mood disorder that is often goes misdiagnosed or undiagnosed. Recently, machine learning techniques have been combined with neuroimaging methods to aid in the diagnosis of BPD. However, most studies have focused on the construction of classifiers based on single-modality MRI. Hence, in this study, we aimed to construct a support vector machine (SVM) model using a combination of structural and functional MRI, which could be used to accurately identify patients with BPD.

Methods In total, 44 patients with BPD and 36 healthy controls were enrolled in the study. Clinical evaluation and MRI scans were performed for each subject. Next, image pre-processing, voxel-based morphometry (VBM), and ReHo analyses were performed. The grey matter volumes or ReHo values of the clusters showed significant differences as discriminant features in the SVM classification model. Based on extracted features, the SVM model was established, and discriminant analysis was performed.

Results After using the two-sample t-test with multiple comparisons, 12 clusters with significant differences were extracted from the data. Next, we used both VBM and ReHo data to construct the new SVM classifier, which could effectively identify patients with BPD at an accuracy of 90% in the test data ($p=0.0014$). Limitations The sample size was small, and we were unable to eliminate the potential effects of medications.

Conclusions A combination of structural and functional MRI can be of added value in the construction of SVM classifiers to aid in the accurate identification of BPD in the clinic.

1. Introduction

Bipolar disorder (BPD) is a chronic and disabling mood disorder found in up to 2.5% of the population. It is characterized by extreme fluctuations in mood, functionality, and energy, in addition to recurrent depressive and manic/hypomanic episodes. Due to the early onset of the disease, high rates of self-inflicted injury and hospitalization, and the negative stigma of BPD, the disease causes significant social and economic burden [1–2]. It was previously reported that the risk of suicide was 20-times higher in patients with BPD than the more general population [3]. In addition, the clinical symptoms of BPD overlap with those of many other mood disorders, including major depressive disorder (MDD), schizophrenia, and attention deficit and hyperactivity disorder (ADHD) [4]. Due to the similar symptom profiles, BPD often goes undiagnosed or misdiagnosed for extended periods. In some cases, it may take up to 10 years after initially seeking treatment to be correctly diagnosed with BPD [5]. This further aggravates the effective treatment of BPD and results in increased disease burden. Hence, researchers are seeking new potential biomarkers to assist the diagnosis and therapeutic monitoring of BPD. Among the new biomarkers, neuroimaging biomarkers have shown excellent potential.

Magnetic resonance imaging (MRI) is a non-invasive neuroimaging technique used to assess the internal anatomy of the brain. In recent years, MRI has been extensively utilized in neuroimaging studies as a

potential biomarker. For structural MRI, voxel-based morphometry (VBM) is one of the most common techniques used to assess focal differences in brain anatomy. The MRI scans of individuals are normalized to a standard template, and voxel-by-voxel comparisons are used to investigate localized abnormalities in gray matter density or volume [6]. For functional MRI, regional homogeneity (ReHo) is a data-driven and highly established approach to evaluate local activity in the brain while at rest. In practice, ReHO represents the temporal homogeneity of the regional blood oxygen level-dependent (BOLD) signal by using Kendall's coefficient of concordance (KCC), which is a number from 0 to 1 that indicates interrater agreement [7]. Fluctuations in ReHo are indicative of local abnormalities in brain activity [8]. Through both VBM and ReHo studies, BPD has been identified as a disorder with several morphological and functional brain abnormalities. However, there have been some inconsistencies between the studies. In terms of VBM studies, abnormalities have been detected extensively throughout the brain, including the frontal lobe, temporal lobe, parietal lobe, cingulate cortex, and the cerebellum. In addition, some of these findings have contradicted each other. For example, some studies shown increased gray matter volumes in the ventral prefrontal cortex (PFC) [9], inferior frontal gyrus [10–11], middle temporal gyri and left temporal pole [12], cingulate gyrus [9, 13], putamen [14–15], and cerebellum [15], while other studies found reduced gray matter volumes in the same areas [16–24]. A similar situation exists with the ReHo analysis. Some studies found increased ReHo values in the frontal lobe, cingulate cortex, and parahippocampal gyrus, while others found reduced ReHo values in the same areas [25–29]. As most of the studies mentioned above were performed at the group level, it is challenging to apply these findings to the individual identification of BPD.

Recently, machine learning approaches have introduced to address the dilemma of inconsistencies. In machine learning, the nature of the "diagnosis" is a classification problem. Among them, Support Vector Machines (SVM) have been developed from the theory of limited samples Statistical Learning Theory (SLT) by Vapnik et al., which was originally designed for binary classification [30]. It is constructed based on the simplicity of structural risk minimization instead of empirical risk minimization. This enables SVM an optimal generalization ability in difficult situations [31–32]. For these reasons, it has been widely used in the detection of mental disorders. For structural MRI, SVM has been used to accurately identify Alzheimer's disease (AD), autism spectrum disorders (ASD), MDD, obsessive-compulsive disorder (OCD), and schizophrenia [33–37]. SVM has also been used to accurately identify different mental disorders in functional MRI studies [38–40]. In terms of BPD, Redlich and colleagues previously used an SVM algorithm based on the whole-brain gray matter to distinguish between BPD and unipolar depression with an accuracy of almost 76% ($p < 0.001$) [41]. In another study, SVM was used in combination with thalamic seed-based connectivity to differentiate between BPD and healthy controls (HC) with an accuracy of 61.7% ($p < 0.038$)[42].

However, the majority of previous studies have used single-modality MRI, either structural or functional MRI. However, a single imaging modality only provides a limited snapshot of the brain in terms of structure or function, while the combined structure-function analysis may provide a more comprehensive perspective of the brain. In recent years, multimodality MRI has been applied to SVM for the classification of schizophrenia and ASD, and the findings have verified that multimodality imaging is significantly more

accurate than single modality imaging [43–44]. Hence, in this study, we have constructed an SVM model, with VBM and ReHo measurement in gray matter volumes as features, to differentiate between patients with BPD from the HCs. We evaluated the classification capabilities of the model and identified the brain areas critical for discriminating between BPD and the HCs. To the best of our knowledge, this is the first study to distinguish between patients with BPD and HCs using an SVM classifier based on the combination of ReHo and VBM analyses.

2. Methods

2.1. Participants

Between January 2012 and December 2015, 44 patients with BPD and 36 age- and sex-matched HCs were recruited from the Affiliated Brain Hospital of Guangzhou Medical University (Guangzhou Huiai Hospital, Guangdong, China) and surrounding communities, respectively. The patients were preliminarily diagnosed as having BPD by one or more of our senior psychiatrists, based on the criteria outlined by the Diagnostic and Statistical Manual of Mental Disorders 4th Edition (DSM-IV) and the structured clinical interview for DSM-IV (SCID) for further confirmation. The HCs were also screened with SCID to ensure they had a fit mental status. All participants were from the Han population, right-handed, and had intelligence quotient (IQ) scores above 75. The exclusion criteria for the BPD and HC groups were as follows: (1) comorbid Axis I or Axis □ disease; (2) history of other psychiatric or neurological illness or severe physical illness; (3) active substance abuse or addiction; (4) unable to complete MRI session due to physical or mental limitations; (5) organic brain lesions detecting by MRI. The study was approved by institutional review boards of Guangzhou Huiai Hospital, and written informed consent was obtained from each participant or their legal guardians before the study.

2.2. Collection of demographic and clinical information

General demographic information, such as age, sex, and years of education, were collected using a pre-designed standardized form. Clinical data, including duration of illness, recurrence, medication, and clinical symptom ratings, were obtained from patients in the BPD group. The Young Mania Rating Scale (YMRS), Positive and Negative Syndrome Scale (PANSS), Hamilton Depression Rating Scale (HAMD), Hamilton Anxiety Table (HAMA), and Global Assessment Function (GAF) were applied to evaluate each subject.

2.3. MRI acquisition

MRI scans were obtained for all of the subjects by a skilled medical imaging technician on the Philips Achieva 3.0T X-series MRI scanner with 8-channel phased array coils at Guangzhou Huiai Hospital. Conventional T1, T2, and blood oxygenation level-dependent (BOLD) images were acquired for each subject. First, 3D T1-weighted volumetric structural images were acquired using a turbo field echo (TFE)-3D T1 sequence with the following parameters: repetition time (TR) = 8.2 msec, echo time (TE) = 3.8

msec, matrix size = 256 × 256, field of view (FOV) = 250 × 250 mm^2, number of slices = 188, slice thickness = 1 mm, and inter-slice gap = 0 mm.

Blood oxygenation level-dependent (BOLD) functional images were acquired using a fast field echo (FFE) echo-planar images (EPI) sequence with the following parameters: TR = 2000 msec, TE = 30 msec, flip angle = 30°, slice numbers = 33, matrix size = 64 × 64, FOV = 220 × 220 × 150 mm^3, inter-slice gap = 0.6 mm, and voxel size = 3.44 × 3.44 × 4 mm. During the fMRI scan time of 523 sec, 240 volumes were obtained. Before the scan, the subjects were instructed to "remain still, relaxed, and close eyes but not fall asleep. Try not to think actively." After the scan, the subjects were asked to confirm that they remained awake during the scanning session.

2.4. Pre-processing and analysis of the structural and functional images

For the structural images, we used the CAT 12 toolbox (http://dbm.neuro.uni-jena.de/cat/) based on the statistic parametric mapping software package (SPM12, http://www.fil.ion.ucl.ac.uk/spm/) in the MATLAB environment (MATLAB 2018b, MathWorks, Natick, MA, USA) to accomplish the data pre-processing and analysis. First, a customized template based on our subjects was created with the segment function in CAT12 and Diffeomorphic Anatomical Registration using Exponentiated Lie (DARTEL) algebra function in SPM 12 [45]. Next, the customized template was used to normalize each subject with a 1.5 × 1.5 × 1.5 mm^3 voxel size. The normalized images were sent through the standard segmentation and modulation procedure using the default settings in CAT 12 toolbox. Lastly, an 8-mm full-width-half maximum (FWHM) Gaussian smoothing was performed to improve the signal-to-noise ratio (SNR). All images were checked for potential image defects or abnormalities.

For the functional images, we used the DPABI_v4.4 (http://www.rfmri.org/dpabi), and SPM12 toolboxes running on MATLAB 2018b were applied to pre-process functional images [46]. First, the first ten time points were discarded to maintain a steady signal. A total of 230 images for each subject were obtained and sliced for time correction. Next, using the realign function in DPABI, we corrected the head motion, and anyone with head motions that exceeded 1.5 mm or rotations over 1.5° were excluded. Subsequently, several spurious covariates, including the linear trend of data, white matter, cerebrospinal fluid, and the Friston-24 parameters of head motion, were removed to reduce the effects of scanning time, breathing, and heart beats [47]. Next, the images were normalized to standard Montreal Neurological Institute (MNI) space, resampling to 3 × 3 × 3 mm^3, based on the previous customized DARTEL template. In the last step of pre-processing, temporal band-pass filtering (0.01–0.08 Hz) was performed to minizine the effects of low-frequency drift and high-frequency physiological noise.

We also used the DPABI toolbox to conduct an H3 ReHo analysis. First, the ReHo map was obtained by calculating Kendall's correlation coefficient (KCC) for each voxel and the 26 adjacent voxels. Next, the ReHo map was normalized by dividing the averaged KCC of the entire brain. Lastly, a 6-mm FWHM Gaussian smoothing was performed in the normalized ReHo map.

2.5. Feature selection and construction of the support vector machine (SVM)

To obtain more sensitive features and improve the stability and efficiency of the classification in the SVM, a two-sample t-test with multiple comparisons was used in the VBM and ReHo statistical analyses [48]. In the VBM analysis, we applied age, sex, education level, and total intracranial volume as nuisance covariates, and the t-map was corrected for multiple comparisons using the Gaussian random field (GRF) theory with a voxel significance of $p < 0.001$ and cluster significance of $p < 0.05$. The grey matter volumes of the clusters showing significant differences were obtained from each subject using the DPABI toolbox. In the ReHo analysis, age, sex, and education level were regarded as nuisance covariates, and the t-map was corrected using the GRF approach with a voxel significance of $p < 0.01$ and cluster significance of $p < 0.05$. The ReHo values of each subject in the clusters showing significant differences were also extracted using the DPABI toolbox. Grey matter volumes and ReHo values in each cluster were selected as feature vectors for discrimination and inputted into the SVM to construct the final classification model.

The classification model, which is based on the support vector machine (SVM), was constructed using the LIBSVM soft package in MATLAB environment. All subjects were randomly divided into the training data and test data, where training data were used to learn the difference between groups and build the classification model, and test data were used to evaluate the classification power of the new model. In this process, leave-one-out cross-validation (LOOCV) and grid search methods were applied to ensure the stability and reliability of the model. Next, the accuracy, specificity, sensitivity, and AUC were assessed to comprehensively evaluate the classification model using a permutation test of 5,000 times. Also, we compared the performance of the classification model with grey matter volumes alone and ReHo value alone, and with the combination of both grey matter volumes and ReHo.

3. Results

3.1. Demographic and clinical information of subjects

In this study, 44 patients diagnosed with BPD and age- and sex-matched 36 healthy controls were recruited. All subjects went through the SCID, and their images were assessed for quality control. None of the subjects were excluded for mental abnormalities, other than BPD, or other defects found in the scans. Demographic and clinical characteristics are summarized in Table 1. In terms of demographics, no significant differences were found in age or gender between the BPD and HC groups ($p > 0.05$), while the length of education was shorter in the BPD group as compared with the HC group. In the BPD group, the age at first onset of the disease was 21.0 ± 5.85, with a disease course of 2.82 ± 1.86 years and recurrence of 1.73 ± 1.19 times. In addition, significant differences in the GAF, HAMA, HAMD, and PANSS scores were found between the BPD group and HC group ($p < 0.05$).

Table 1

Demographic and clinical characteristics of subjects in the BPD and HC groups.

	BPD	HC	t/x<	P
Age	23.11 ± 5.15	22.78 ± 2.45	0.3589	0.72
Sex	18/26	22/14	3.2323	0.072
Education (years)	12.59 ± 2.94	15.19 ± 1.62	-4.7485	< 0.001
Onset-year	21.3 ± 5.85	-	-	-
Course of disease	2.82 ± 1.86	-	-	-
Recurrence	1.73 ± 1.19	-	-	-
GAF	75.95 ± 14.36	98.86 ± 2.88	-9.410	< 0.001
HAMA	3.64 ± 3.69	0.42 ± 0.65	5.170	< 0.001
HAMD	2.91 ± 3.85	0.39 ± 0.80	3.860	< 0.001
PANSS				
PANSS-P	9.48 ± 4.29	7.14 ± 0.62	3.228	0.002
PANSS-N	8.50 ± 2.49	7.03 ± 0.29	3.521	0.001
PANSS-G	21.86 ± 6.49	16.38 ± 0.78	5.037	< 0.001
PANSS-Total	41.07 ± 11.87	30.47 ± 1.09	5.335	< 0.001
YOUNG	3.84 ± 7.10	0.03 ± 0.17	3.218	0.002

BPD, bipolar disorder; HC, healthy controls; GAF, Global Assessment Function; HAMA, Hamilton Anxiety Table; HAMD, Hamilton Depression Rating Scale; PANSS, Positive and Negative Syndrome Scale; PANSS-P, PANSS-positive; PANSS-N, PANSS-Negative; PANSS-G, PANSS-General; YMRS, Young Mania Rating Scale.

3.2. Feature selection

For the VBM analysis, A total of 12 clusters showed significant differences between the groups and were extracted. The 12 clusters covered the bilateral inferior frontal gyrus, precentral gyrus, postcentral gyrus, middle occipital gyrus, fusiform and right middle frontal gyrus, cingulate gyrus, anterior cingulate, hippocampus, superior temporal gyrus, lingual gyrus and left limbic lobe, inferior temporal gyrus, and precuneus (corrected voxel significance $p < 0.001$, cluster significance $p < 0.05$, Table 2 and Fig. 1). The specific grey matter volumes of these clusters were extracted and shown in Table S1 (Supplementary Materials).

Table 2

Clusters showing significant differences between the BPD and HC groups in gray matter volumes.

Cluster number	Brain regions	Peak MNI coordinate			Voxel sizes	T
		x	y	z		
1	Right superior temporal gyrus Right hippocampus Right fusiform	45	-20	-14	891	-5.15
2	Right lingual gyrus	15	-89	-14	123	-3.96
3	Left inferior temporal gyrus Left fusiform	-42	-44	-3	456	-4.38
4	Left inferior frontal gyrus	-21	35	0	269	-4.23
5	Right inferior frontal gyrus Right middle frontal gyrus	30	35	-3	352	-4.31
6	Right Precentral Gyrus Right Middle Frontal Gyrus Right Postcentral	33	-11	30	1504	-5.31
7	Left Precentral Gyrus Left Postcentral Gyrus	-54	-15	28	851	-4.34
8	Left Limbic Lobe	-20	20	23	814	-5.14
9	Right Cingulate Gyrus Right Anterior Cingulate	20	3	33	696	-4.40
10	Right Middle occipital gyrus	35	-66	29	381	-4.16
11	Left Precuneus Left Middle occipital gyrus	-15	-59	36	489	-4.71
12	Right Cingulate Gyrus	9	-32	35	114	-3.92

MNI, Montreal Neurological Institute

For the ReHo analysis, significant differences were detected in two clusters, including the right medial frontal gyrus, anterior cingulate, left lentiform nucleus, and putamen between the BPD group and HC group (corrected voxel significance $p < 0.01$, cluster significance $p < 0.05$, Table 3 and Fig. 2). The ReHo values of the two clusters were extracted and shown in Table S2 (Supplementary Materials).

Table 3

Clusters showing significant differences between the BPD and HC groups in ReHo values.

Cluster number	Brain regions	Peak MNI coordinate			Voxel sizes	T
		x	y	z		
1	Left Lentiform Nucleus Left Putamen	-27	6	27	631	4.34
2	Right Medial Frontal Gyrus Right Anterior Cingulate	9	-48	45	648	-4.94
MNI, Montreal Neurological Institute						

3.3. SVM analysis

Based on a combination of grey matter volume differences and ReHo values, the trained SVM classifier could correctly identify BPD with an accuracy of 90%, sensitivity of 86.36%, and specificity of 94.4% in the test data (p = 0.0014). The specific classification results from the test data are shown in Fig. 3. Based on grey matter volumes alone, the accuracy was reduced to 75%, with a sensitivity of 68.18% and a specificity of 83.33% (p = 0.0044). Similarly, when based on ReHo values alone, the accuracy was reduced to 80%, with increased sensitivity of 95.45% and specificity of 61.11%. As shown in Fig. 4, the area under the receiver operating characteristic (ROC) curves (AUC) of the three SVM classifiers were 0.949, 0.803, and 0.871, respectively.

4. Discussion

To the best of our knowledge, this is the first study to demonstrate the detection of individual patients with BPD using SVM classifiers based on a combination of ReHo values and grey matter volumes. We constructed the SVM classifier, which could classify BPD with an AUC of 0.949. Our findings showed that the SVM classifier based on a combination of the two performed better than the SVM classifiers based on gray matter volumes alone (AUC = 0.803) and ReHo values alone (AUC = 0.871). This result supports our previous hypothesis that the combination of structural and functional MRI could improve the recognition of BPD using an SVM classifier. Similar findings have been detected by other research groups. Using multimodality MRI, several studies have constructed SVM classifiers for the identification of ASD, Alzheimer's Disease, and schizophrenia [43, 49–50]. Beyond this, some researchers have combined multimodality MRI with other characteristics of these diseases, such as cerebral spinal fluid, electroencephalography, and eye-tracking [51–52]. However, markers selection requires careful consideration, as it has been shown that too much data may not improve the power of the SWM classifier in some instances[53]. The finding may be due to the process of overfitting in machine learning, which may reduce the generalization of the classifier.

In this present study, grey matter volumes and ReHo values were chosen to build the classifiers. Both VBM and ReHo analyses reflect local abnormalities of the brain, in terms of structure and function dimensions independently. In addition, the two approaches are data-driven measurements, which are independent from preconceived assumptions and could make the findings more objective. In the VBM analyses, reduced grey matter volumes were confirmed in multiple areas of the frontal lobe, which may be due to the important processes in nonverbal function and emotional stimuli [17, 54]. As for the cingulate, anterior cingulate, limbic cortex, and hippocampus, these are critical areas involving emotional processing, memory, and executive functioning [55]. The reductions of grey matter volumes in these areas were observed in the present study and are consistent with previous reports. Besides, the superior temporal gyrus is also associated with emotional processing, and is thought one of the primary alterations in patients with BPD type I [56–59]. The reductions in grey matter volume of the inferior temporal gyrus may be due to our sample size consisting of mostly BPD type I patients. In the ReHo analyses, increases in ReHo were detected in the left putamen and lentiform nucleus in the current study. To our knowledge, this change was first observed in the ReHo analysis of patients with BPD, which may be the primary change in patients with BPD and has been supported the VBM analyses [59].

Most of the findings from the VBM and ReHo analyses in the present study have been found in previous studies [12, 16–17, 20, 25, 54, 60–61]. However, due to some opposition from other studies [12–13, 24, 28, 62], the identification of these abnormalities as biomarkers may be preliminary. Thus, we constructed an SVM classifier with excellent performance in the identification of individual patients with BPD patients with an accuracy of approximately 90%. Besides, using the combination of grey matter volumes and ReHo values to construct the SVM classifier, the design performed better than using either gray matter volumes or ReHo values individually. These results support our hypothesis that the combination of structural and functional MRI with an SVM classifier may aid in the detection of BPD in the clinic.

Also, there are some limitations to the present study. This is a small and non-prospective study, with poor generalization and low confidence. Thus, we performed the leave-one-out cross-validation to improve the reliability and stability of the classifier. Besides, the theoretical basis of the SVM is structural risk minimization instead of empirical risk minimization, which can effectively work with some degree of error and does not require a large sample size. Another key limitation of the current study is potential drug-bias. Due to ethical reasons, all patients in this study were receiving medications. Hence, it can be difficult to distinguish whether the VBM and ReHo analysis findings are medication-induced or abnormalities detected in the disease itself. A further distinction may be needed using unmedicated patients with long-term follow-ups. Lastly, this study focused on grey matter volumes and ReHo values as discriminant features to construct the SVM classifier, yet these may not provide a comprehensive assessment of the brain. More suitable neuroimaging biomarkers, such as those to detect changes in white matter microstructures and cerebral blood flow, should be considered in future studies.

5. Conclusions

In this study, we have shown grey matter volumes and ReHo values, as the discriminate features, could be used to conduct SVM classifiers and recognize patients with BPD at the individual level. Compared with the single-modality MRI, the combination of structural and functional MRI data could be of added value in the construction of SVM classifiers for the accurate detection of BPD.

Declarations

Funding: The study was supported by the Science and Technology Planning Project of Guangdong Province, China (2013B021800074) and the Southern China International Cooperation Base for Early Intervention and Functional Rehabilitation of Neurological Diseases (2015B050501003), Guangdong Provincial Engineering Center For Major Neurological Disease Treatment, Guangdong Provincial Translational Medicine Innovation Platform for Diagnosis and Treatment of Major Neurological Disease, Guangdong Provincial Clinical Research Center for Neurological Diseases

Conflicts of Interest: The authors declare no potential conflicts of interest.

Data availability statement: The data used to support the findings of this study are available from the corresponding author upon request.

References

[1] J. Alonso, M. Petukhova, G. Vilagut, S. Chatterji, S. Heeringa, T.B. Üstün, A.O. Alhamzawi, M.C. Viana, M. Angermeyer, E. Bromet, R. Bruffaerts, G. de Girolamo, S. Florescu, O. Gureje, J.M. Haro, H. Hinkov, C.Y. Hu, E.G. Karam, V. Kovess, D. Levinson, M.E. Medina-Mora, Y. Nakamura, J. Ormel, J. Posada-Villa, R. Sagar, K.M. Scott, A. Tsang, D.R. Williams, R.C. Kessler, Days out of role due to common physical and mental conditions: results from the WHO World Mental Health surveys, Mol. Psychiatry, 16 (2011) 1234-46.

[2] G.E. Simon, Social and economic burden of mood disorders, Biol. Psychiatry, 54 (2003) 208-15.

[3] M. Pompili, X. Gonda, G. Serafini, M. Innamorati, L. Sher, M. Amore, Z. Rihmer, P. Girardi, Epidemiology of suicide in bipolar disorders: a systematic review of the literature., 2013, pp. 457-490.

[4] L.L. Pendergast, E.A. Youngstrom, K.G. Merkitch, K.A. Moore, C.L. Black, L.Y. Abramson, L.B. Alloy, Differentiating bipolar disorder from unipolar depression and ADHD: the utility of the general behavior inventory., 2014, pp. 195-206.

[5] R.M. Hirschfeld, L. Lewis, L.A. Vornik, Perceptions and impact of bipolar disorder: how far have we really come? Results of the national depressive and manic-depressive association 2000 survey of individuals with bipolar disorder, J Clin Psychiatry, 64 (2003) 161-74.

[6] J. Ashburner, K.J. Friston, Voxel-based morphometry--the methods, NEUROIMAGE, 11 (2000) 805-21.

[7] Y. Zang, T. Jiang, Y. Lu, Y. He, L. Tian, Regional homogeneity approach to fMRI data analysis, NEUROIMAGE, 22 (2004) 394-400.

[8] Q.Z. Wu, D.M. Li, W.H. Kuang, T.J. Zhang, S. Lui, X.Q. Huang, R.C. Chan, G.J. Kemp, Q.Y. Gong, Abnormal regional spontaneous neural activity in treatment-refractory depression revealed by resting-state fMRI, HUM BRAIN MAPP, 32 (2011) 1290-9.

[9] C.M. Adler, A.D. Levine, M.P. DelBello, S.M. Strakowski, Changes in gray matter volume in patients with bipolar disorder, Biol. Psychiatry, 58 (2005) 151-7.

[10] A. Sarıçiçek, N. Yalın, C. Hıdıroğlu, B. Çavuşoğlu, C. Taş, D. Ceylan, N. Zorlu, E. Ada, Z. Tunca, A. Özerdem, Neuroanatomical correlates of genetic risk for bipolar disorder: A voxel-based morphometry study in bipolar type I patients and healthy first degree relatives, J Affect Disord, 186 (2015) 110-8.

[11] A.C. Stanfield, T.W.J. Moorhead, D.E. Job, J. McKirdy, J.E.D. Sussmann, J. Hall, S. Giles, E.C. Johnstone, S.M. Lawrie, A.M. McIntosh, Structural abnormalities of ventrolateral and orbitofrontal cortex in patients with familial bipolar disorder., 2009, pp. 135-144.

[12] M. Haldane, G. Cunningham, C. Androutsos, S. Frangou, Structural brain correlates of response inhibition in Bipolar Disorder I, J. Psychopharmacol. (Oxford), 22 (2008) 138-43.

[13] C.M. Adler, M.P. DelBello, K. Jarvis, A. Levine, J. Adams, S.M. Strakowski, Voxel-based study of structural changes in first-episode patients with bipolar disorder., 2007, pp. 776-781.

[14] Z. Chen, L. Cui, M. Li, L. Jiang, W. Deng, X. Ma, Q. Wang, C. Huang, Y. Wang, D.A. Collier, Q. Gong, T. Li, Voxel based morphometric and diffusion tensor imaging analysis in male bipolar patients with first-episode mania, Prog. Neuropsychopharmacol. Biol. Psychiatry, 36 (2012) 231-8.

[15] L. Cui, M. Li, W. Deng, W. Guo, X. Ma, C. Huang, L. Jiang, Y. Wang, D.A. Collier, Q. Gong, T. Li, Overlapping clusters of gray matter deficits in paranoid schizophrenia and psychotic bipolar mania with family history, NEUROSCI LETT, 489 (2011) 94-8.

[16] J.R. Almeida, D. Akkal, S. Hassel, M.J. Travis, L. Banihashemi, N. Kerr, D.J. Kupfer, M.L. Phillips, Reduced gray matter volume in ventral prefrontal cortex but not amygdala in bipolar disorder: significant effects of gender and trait anxiety, Psychiatry Res, 171 (2009) 54-68.

[17] Y. Cai, J. Liu, L. Zhang, M. Liao, Y. Zhang, L. Wang, H. Peng, Z. He, Z. Li, W. Li, S. Lu, Y. Ding, L. Li, Grey matter volume abnormalities in patients with bipolar I depressive disorder and unipolar depressive disorder: a voxel-based morphometry study, NEUROSCI BULL, 31 (2015) 4-12.

[18] G.G. Brown, J.S. Lee, I.A. Strigo, M.P. Caligiuri, M.J. Meloy, J. Lohr, Voxel-based morphometry of patients with schizophrenia or bipolar I disorder: a matched control study, Psychiatry Res, 194 (2011) 149-56.

[19] H. Tost, M. Ruf, C. Schmäl, T.G. Schulze, C. Knorr, C. Vollmert, K. Bösshenz, G. Ende, A. Meyer-Lindenberg, F.A. Henn, M. Rietschel, Prefrontal-temporal gray matter deficits in bipolar disorder patients with persecutory delusions, J Affect Disord, 120 (2010) 54-61.

[20] L.N. Yatham, I.K. Lyoo, P. Liddle, P.F. Renshaw, D. Wan, R.W. Lam, J. Hwang, A magnetic resonance imaging study of mood stabilizer- and neuroleptic-naïve first-episode mania, BIPOLAR DISORD, 9 (2007) 693-7.

[21] S. Haller, A. Xekardaki, C. Delaloye, A. Canuto, K.O. Lövblad, G. Gold, P. Giannakopoulos, Combined analysis of grey matter voxel-based morphometry and white matter tract-based spatial statistics in late-life bipolar disorder, J Psychiatry Neurosci, 36 (2011) 391-401.

[22] F. Wang, J.H. Kalmar, F.Y. Womer, E.E. Edmiston, L.G. Chepenik, R. Chen, L. Spencer, H.P. Blumberg, Olfactocentric paralimbic cortex morphology in adolescents with bipolar disorder, BRAIN, 134 (2011) 2005-12.

[23] K. Narita, M. Suda, Y. Takei, Y. Aoyama, T. Majima, M. Kameyama, H. Kosaka, M. Amanuma, M. Fukuda, M. Mikuni, Volume reduction of ventromedial prefrontal cortex in bipolar II patients with rapid cycling: a voxel-based morphometric study, Prog. Neuropsychopharmacol. Biol. Psychiatry, 35 (2011) 439-45.

[24] S. Frangou, Brain structural and functional correlates of resilience to Bipolar Disorder., 2011, pp. 184.

[25] X. Yao, Z. Yin, F. Liu, S. Wei, Y. Zhou, X. Jiang, Y. Wei, K. Xu, F. Wang, Y. Tang, Shared and distinct regional homogeneity changes in bipolar and unipolar depression, NEUROSCI LETT, 673 (2018) 28-32.

[26] C.H. Liu, X. Ma, F. Li, Y.J. Wang, C.L. Tie, S.F. Li, T.L. Chen, T.T. Fan, Y. Zhang, J. Dong, L. Yao, X. Wu, C.Y. Wang, Regional homogeneity within the default mode network in bipolar depression: a resting-state functional magnetic resonance imaging study, PLOS ONE, 7 (2012) e48181.

[27] M.J. Liang, Q. Zhou, K.R. Yang, X.L. Yang, J. Fang, W.L. Chen, Z. Huang, Identify changes of brain regional homogeneity in bipolar disorder and unipolar depression using resting-state FMRI, PLOS ONE, 8 (2013) e79999.

[28] W. Gao, Q. Jiao, S. Lu, Y. Zhong, R. Qi, D. Lu, Q. Xiao, F. Yang, G. Lu, L. Su, Alterations of regional homogeneity in pediatric bipolar depression: a resting-state fMRI study, BMC PSYCHIATRY, 14 (2014) 222.

[29] Q. Xiao, Y. Zhong, D. Lu, W. Gao, Q. Jiao, G. Lu, L. Su, Altered regional homogeneity in pediatric bipolar disorder during manic state: a resting-state fMRI study, PLOS ONE, 8 (2013) e57978.

[30] V. Vapnik, The nature of statistical learning theory, Springer science & business media2013.

[31] M.A. Hearst, S.T. Dumais, E. Osuna, J. Platt, B. Scholkopf, Support vector machines, IEEE Intelligent Systems and their applications, 13 (1998) 18-28.

[32] A.I. Belousov, S.A. Verzakov, J. Von Frese, A flexible classification approach with optimal generalisation performance: support vector machines, CHEMOMETR INTELL LAB, 64 (2002) 15-25.

[33] P.P. Oliveira, R. Nitrini, G. Busatto, C. Buchpiguel, J.R. Sato, E. Amaro, Use of SVM methods with surface-based cortical and volumetric subcortical measurements to detect Alzheimer's disease, J ALZHEIMERS DIS, 19 (2010) 1263-72.

[34] C. Ecker, A. Marquand, J. Mourão-Miranda, P. Johnston, E.M. Daly, M.J. Brammer, S. Maltezos, C.M. Murphy, D. Robertson, S.C. Williams, D.G. Murphy, Describing the brain in autism in five dimensions–magnetic resonance imaging-assisted diagnosis of autism spectrum disorder using a multiparameter classification approach, J NEUROSCI, 30 (2010) 10612-23.

[35] B. Mwangi, K.P. Ebmeier, K. Matthews, J.D. Steele, Multi-centre diagnostic classification of individual structural neuroimaging scans from patients with major depressive disorder, BRAIN, 135 (2012) 1508-21.

[36] C. Zhou, Y. Cheng, L. Ping, J. Xu, Z. Shen, L. Jiang, L. Shi, S. Yang, Y. Lu, X. Xu, Support Vector Machine Classification of Obsessive-Compulsive Disorder Based on Whole-Brain Volumetry and Diffusion Tensor Imaging, FRONT PSYCHIATRY, 9 (2018) 524.

[37] Y. Xiao, Z. Yan, Y. Zhao, B. Tao, H. Sun, F. Li, L. Yao, W. Zhang, S. Chandan, J. Liu, Q. Gong, J.A. Sweeney, S. Lui, Support vector machine-based classification of first episode drug-naïve schizophrenia patients and healthy controls using structural MRI, SCHIZOPHR RES, (2017).

[38] J.S. Anderson, J.A. Nielsen, A.L. Froehlich, M.B. DuBray, T.J. Druzgal, A.N. Cariello, J.R. Cooperrider, B.A. Zielinski, C. Ravichandran, P.T. Fletcher, A.L. Alexander, E.D. Bigler, N. Lange, J.E. Lainhart, Functional connectivity magnetic resonance imaging classification of autism, BRAIN, 134 (2011) 3742-54.

[39] L.L. Zeng, H. Shen, L. Liu, L. Wang, B. Li, P. Fang, Z. Zhou, Y. Li, D. Hu, Identifying major depression using whole-brain functional connectivity: a multivariate pattern analysis, BRAIN, 135 (2012) 1498-507.

[40] S. Wang, Y. Zhang, L. Lv, R. Wu, X. Fan, J. Zhao, W. Guo, Abnormal regional homogeneity as a potential imaging biomarker for adolescent-onset schizophrenia: A resting-state fMRI study and support vector machine analysis, SCHIZOPHR RES, 192 (2018) 179-184.

[41] R. Redlich, J.J. Almeida, D. Grotegerd, N. Opel, H. Kugel, W. Heindel, V. Arolt, M.L. Phillips, U. Dannlowski, Brain morphometric biomarkers distinguishing unipolar and bipolar depression. A voxel-based morphometry-pattern classification approach, JAMA PSYCHIAT, 71 (2014) 1222-30.

[42] A. Anticevic, M.W. Cole, G. Repovs, J.D. Murray, M.S. Brumbaugh, A.M. Winkler, A. Savic, J.H. Krystal, G.D. Pearlson, D.C. Glahn, Characterizing thalamo-cortical disturbances in schizophrenia and bipolar illness, CEREB CORTEX, 24 (2014) 3116-30.

[43] B. Sen, N.C. Borle, R. Greiner, M. Brown, A general prediction model for the detection of ADHD and Autism using structural and functional MRI, PLOS ONE, 13 (2018) e0194856.

[44] C. Cabral, L. Kambeitz-Ilankovic, J. Kambeitz, V.D. Calhoun, D.B. Dwyer, S. von Saldern, M.F. Urquijo, P. Falkai, N. Koutsouleris, Classifying Schizophrenia Using Multimodal Multivariate Pattern Recognition Analysis: Evaluating the Impact of Individual Clinical Profiles on the Neurodiagnostic Performance, Schizophr Bull, 42 Suppl 1 (2016) S110-7.

[45] S. Shen, A. Sterr, Is DARTEL-based voxel-based morphometry affected by width of smoothing kernel and group size? A study using simulated atrophy, J MAGN RESON IMAGING, 37 (2013) 1468-75.

[46] C.G. Yan, X.D. Wang, X.N. Zuo, Y.F. Zang, DPABI: Data Processing & Analysis for (Resting-State) Brain Imaging, NEUROINFORMATICS, 14 (2016) 339-51.

[47] K.J. Friston, S. Williams, R. Howard, R.S. Frackowiak, R. Turner, Movement-related effects in fMRI time-series, MAGN RESON MED, 35 (1996) 346-55.

[48] S. Wang, G. Wang, H. Lv, R. Wu, J. Zhao, W. Guo, Abnormal regional homogeneity as potential imaging biomarker for psychosis risk syndrome: a resting-state fMRI study and support vector machine analysis, Sci Rep, 6 (2016) 27619.

[49] J.E. Park, B. Park, S.J. Kim, H.S. Kim, C.G. Choi, S.C. Jung, J.Y. Oh, J. Lee, J.H. Roh, W.H. Shim, Improved Diagnostic Accuracy of Alzheimer's Disease by Combining Regional Cortical Thickness and Default Mode Network Functional Connectivity: Validated in the Alzheimer's Disease Neuroimaging Initiative Set., 2017, pp. 983-991.

[50] J. Lee, M. Chon, H. Kim, Y. Rathi, S. Bouix, M.E. Shenton, M. Kubicki, Diagnostic value of structural and diffusion imaging measures in schizophrenia., 2018, pp. 467-474.

[51] J.L. Shaffer, J.R. Petrella, F.C. Sheldon, K.R. Choudhury, V.D. Calhoun, R.E. Coleman, P.M. Doraiswamy, Predicting cognitive decline in subjects at risk for Alzheimer disease by using combined cerebrospinal fluid, MR imaging, and PET biomarkers, RADIOLOGY, 266 (2013) 583-91.

[52] X. Ding, X. Yue, R. Zheng, C. Bi, D. Li, G. Yao, Classifying major depression patients and healthy controls using EEG, eye tracking and galvanic skin response data, J Affect Disord, 251 (2019) 156-161.

[53] M.H. Nguyen, F. De la Torre, Optimal feature selection for support vector machines, PATTERN RECOGN, 43 (2010) 584-591.

[54] I.K. Lyoo, M.J. Kim, A.L. Stoll, C.M. Demopulos, A.M. Parow, S.R. Dager, S.D. Friedman, D.L. Dunner, P.F. Renshaw, Frontal lobe gray matter density decreases in bipolar I disorder, Biol. Psychiatry, 55 (2004) 648-51.

[55] P.G. Gasquoine, Localization of function in anterior cingulate cortex: from psychosurgery to functional neuroimaging, Neurosci Biobehav Rev, 37 (2013) 340-8.

[56] T. Allison, A. Puce, G. McCarthy, Social perception from visual cues: role of the STS region, Trends Cogn. Sci. (Regul. Ed.), 4 (2000) 267-278.

[57] H.L. Gallagher, C.D. Frith, Functional imaging of 'theory of mind', Trends Cogn. Sci. (Regul. Ed.), 7 (2003) 77-83.

[58] T.H. Ha, K. Ha, J.H. Kim, J.E. Choi, Regional brain gray matter abnormalities in patients with bipolar II disorder: a comparison study with bipolar I patients and healthy controls, NEUROSCI LETT, 456 (2009) 44-8.

[59] X. Lu, Y. Zhong, Z. Ma, Y. Wu, P.T. Fox, N. Zhang, C. Wang, Structural imaging biomarkers for bipolar disorder: Meta-analyses of whole-brain voxel-based morphometry studies, DEPRESS ANXIETY, 36 (2019) 353-364.

[60] M. Li, L. Cui, W. Deng, X. Ma, C. Huang, L. Jiang, Y. Wang, D.A. Collier, Q. Gong, T. Li, Voxel-based morphometric analysis on the volume of gray matter in bipolar I disorder., 2011, pp. 92-97.

[61] C. Liu, X. Ma, X. Wu, Y. Zhang, F. Zhou, F. Li, C. Tie, J. Dong, Y. Wang, Z. Yang, C. Wang, Regional homogeneity of resting-state brain abnormalities in bipolar and unipolar depression., 2013, pp. 52-59.

[62] Q. Xiao, D. Cui, Q. Jiao, Y. Zhong, W. Cao, G. Lu, L. Su, Altered regional homogeneity in pediatric bipolar disorder during manic and euthymic state: a resting-state fMRI study., 2019, pp. 1789-1798.

Figures

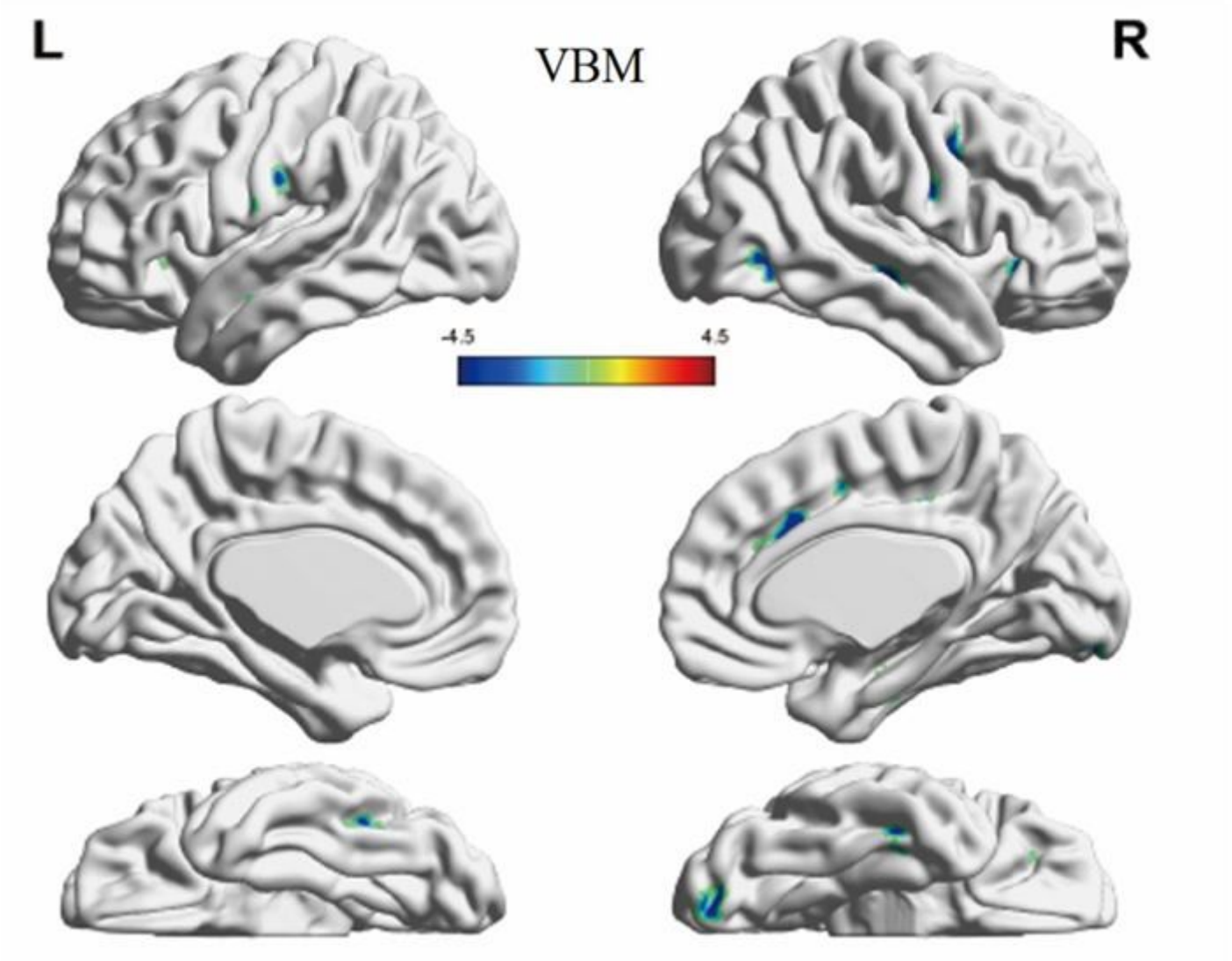

Figure 1

Clusters showing significant differences in between the BPD and HC groups in gray matter volume.

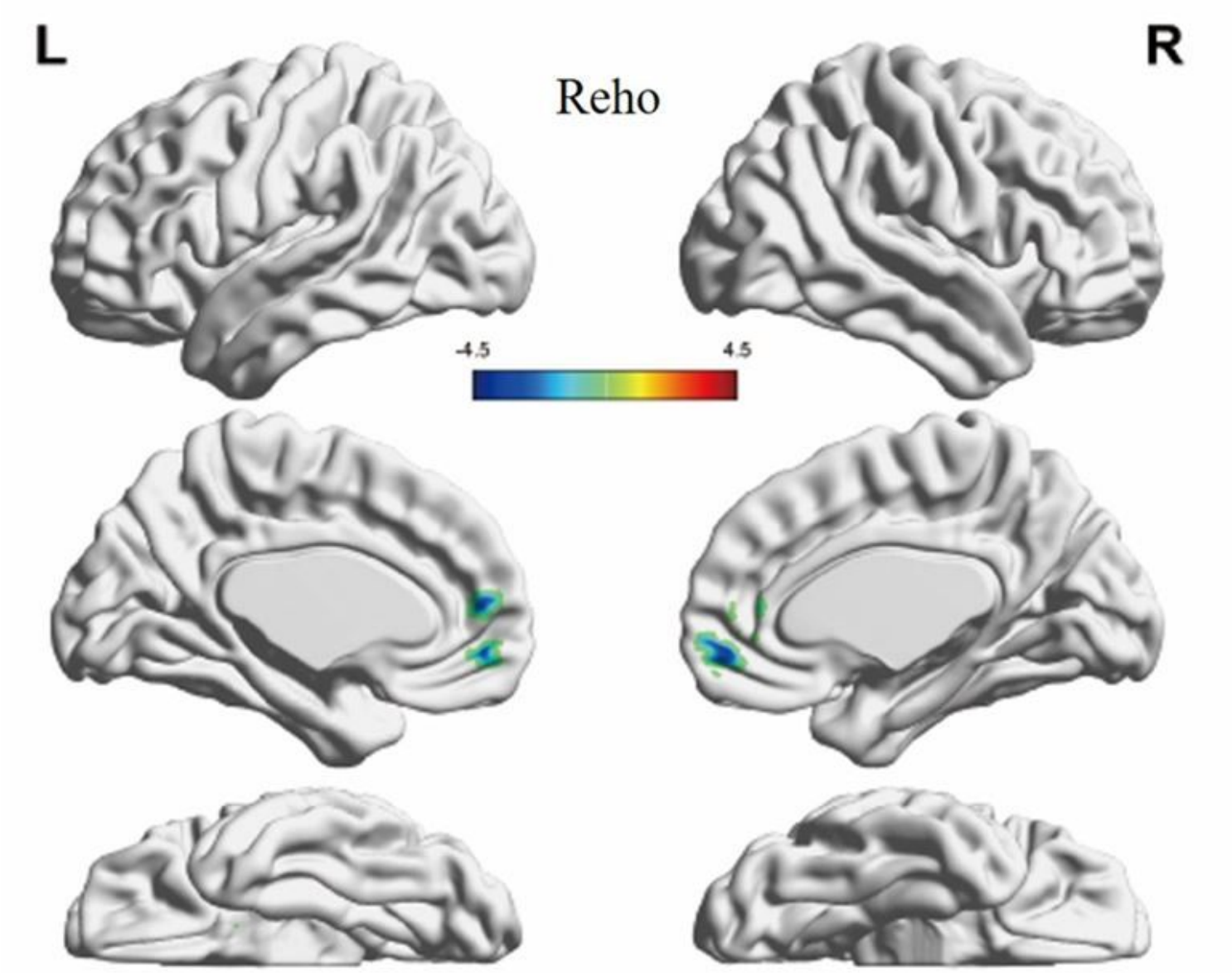

Figure 2

Clusters showing significant differences between the BPD and HC groups in the ReHo values.

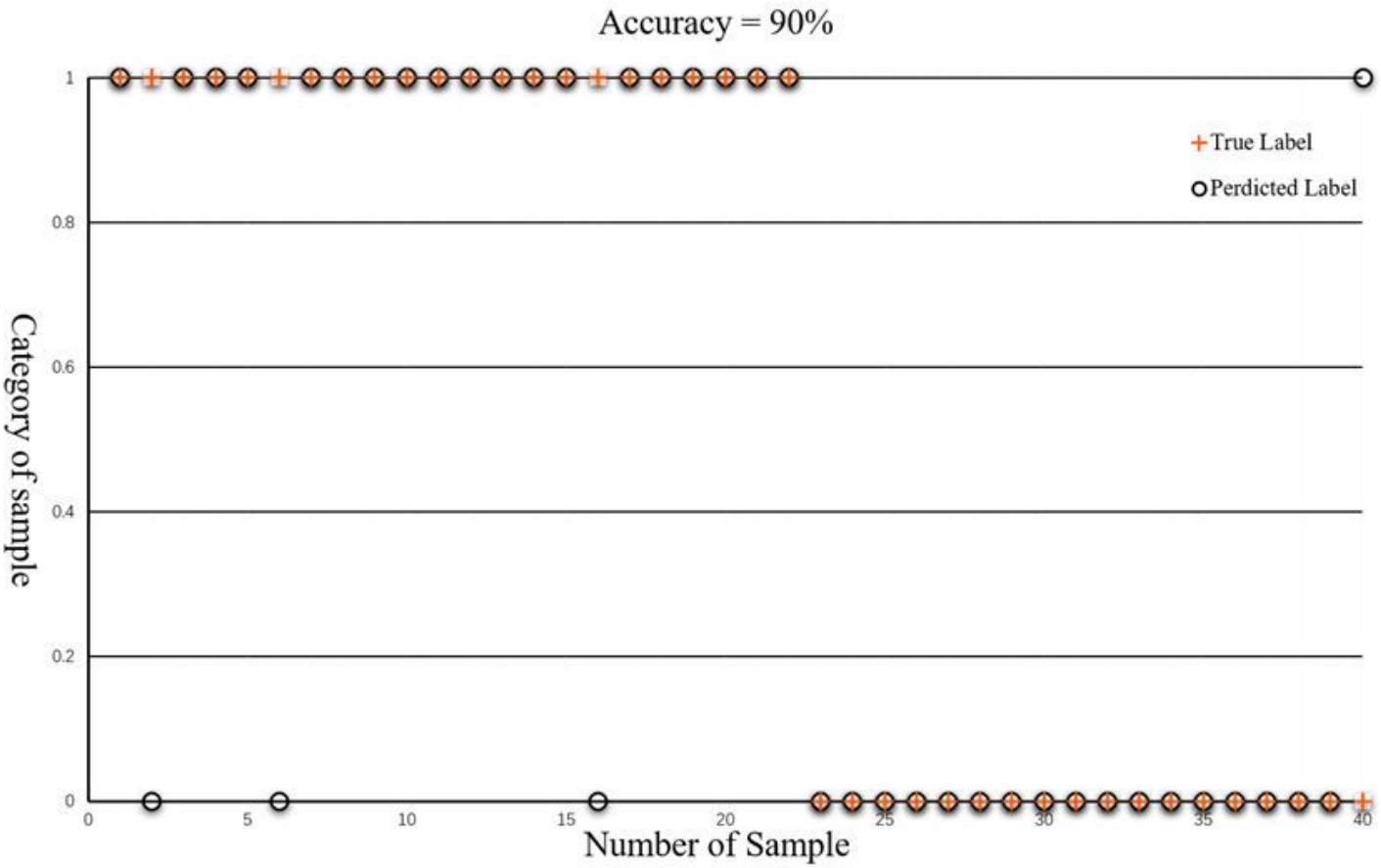

Figure 3

Classification results based on a combination of grey matter volumes and ReHo values.

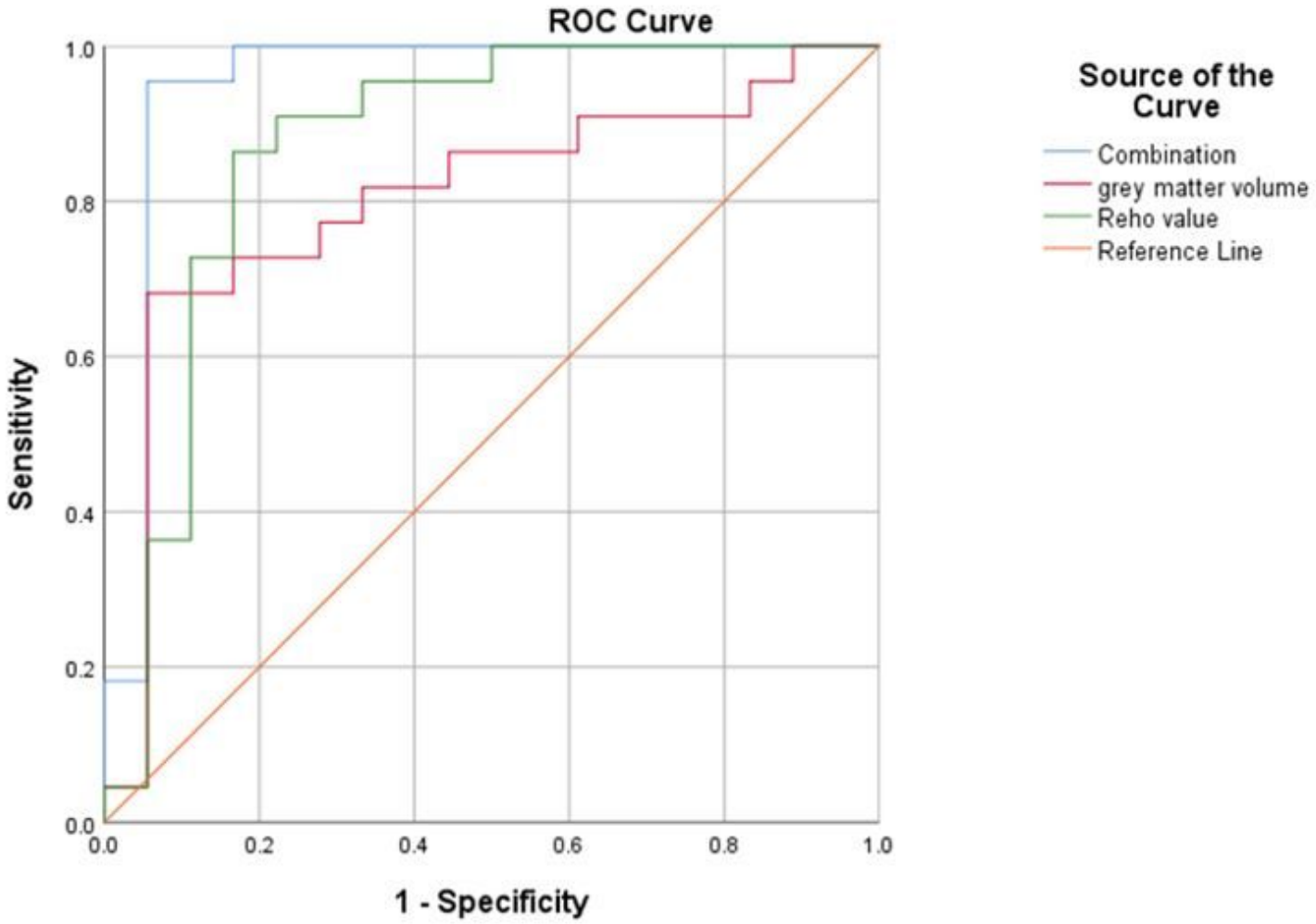

Figure 4

ROC curves showing the performance of the three SVM classifiers.

Supplementary Files

This is a list of supplementary files associated with this preprint. Click to download.

- supplementmaterial.pdf